Design of a Hemispherical Antenna Array Receiver for Medical Applications

Mohammad Safar and Robert W. Newcomb

Department of Electrical & Computer Engineering, University of Maryland, College Park, MD, USA
msafer10@hotmail.com, newcomb@eng.umd.edu

Abstract. A hemispherical antenna array consisting of 42 elements was proposed and simulated. The array is capable of receiving signals at 500 kHz. The array elements are distributed on a hemisphere to be placed on a human's head. The function of the array is to receive brain waves or signals from embedded electronics in the brain. By considering the problem as a boundary valued problem with the source signal or field being in the brain, the induced current on the antenna elements can be determined using boundary conditions. A beamforming technique for reception was used that made use of the orthogonality property of the *transverse electric* fields to enable the array to receive from one or multiple points from within the brain.

Index Terms: Hemispherical array, Boundary valued problem (BVP), Beaamforming.

1 Introduction

Antenna arrays have the ability to receive signals while improving the overall signal-to-noise since they allow for constructive interference in the desired point or direction of reception and destructive interference in all other directions. This property can be put in use when considering medical applications where there is a transmitter embedded inside the body and a receiver is needed to receive signals from that transmitter [1]-[4].

The reception is achieved by using some kind of a beamforming algorithm. This is usually done by first defining or calculating a real property of the signal that will be maximum in the direction where the signal is coming from and all what the designer have to do is try to scan for this maximum using some kind of an optimization scheme. According to [5], the algorithms for direction of arrival (DOA) estimation fall into the following 3 categories: (1) spectral-based algorithm; (2) subspace-based methods & (3) parametric methods. In the literature there are many kinds of reception strategies that fall in the above categories [6]-[13].

J.M. Ferrández et al. (Eds.): IWINAC 2011, Part I, LNCS 6686, pp. 256–265, 2011.
© Springer-Verlag Berlin Heidelberg 2011

In the case presented in this paper the array is a hemispherical array that is placed on the human head (or could be used for any other spherical surface) to receive signals from the brain either as brain waves or from embedded transmitters. A new beamforming technique is used that allows for reception from one or multiple directions.

2 Theoretical Analysis

2.1 Problem Statement

The design of the hemispherical array was done by solving an electromagnetic boundary valued problem in which the human head was modeled as a three layered hemisphere like the one shown in Fig. 1. Of course modeling the head as a perfect hemisphere is an assumption, but a necessary one to enable the use of the spherical coordinate system. The antenna elements are of course fixed onto a helmet which is in turn placed on the head but in the analysis it is assumed that the antennas are placed right above the head to reduce the number of layers and hence simplify the analysis. It is seen from the figure that there are four regions marked as (0), (1), (2) and (3). Region (0) is the outside of the head (i.e. free

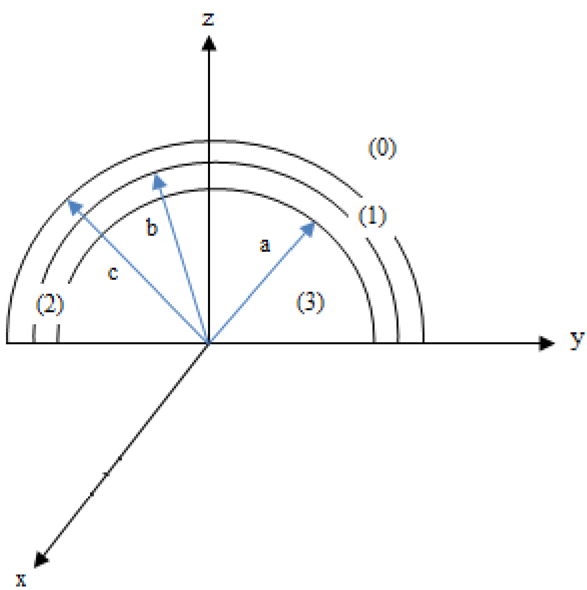

Fig. 1. A simple model of a human's head as seen from the front. There are four regions denoted by (0), (1), (2) and (3) which represent free space, the skull and brain respectively. The radius of the brain is a, while b denotes the radius from the center of the brain to the outer part of the skull and c for skin where the antenna elements are going to be placed.

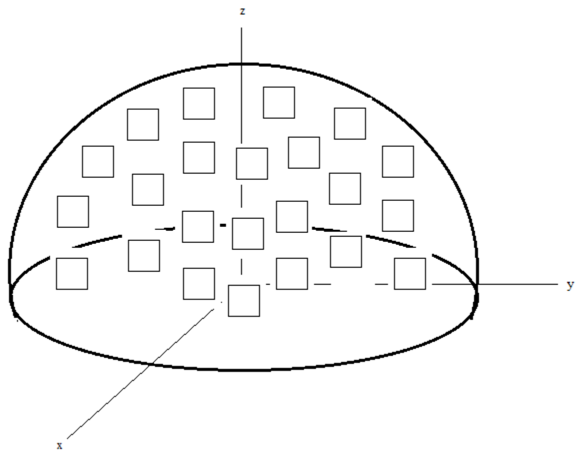

Fig. 2. Loop Antennas Placed on the Human head

space), region (1) is the skin, region (2) is the skull and finally region (3) is the brain. The 42 antennas are going to be placed on top of the skin surface and they will cover a hemispherical surface of radius c (Fig. 2).

Since the human head is approximated to be spherical, it is therefore obvious that the boundary value problem will be solved by utilizing the spherical coordinate system. According to [14, ch.6-1], any electromagnetic problem with spherical symmetry can be solved using the electric vector potential F_r and the magnetic vector potential A_r in spherical coordinates. Any electromagnetic wave can be decomposed into two orthogonal sets of functions which are the *transverse electric (TE)* F_r and the *transverse magnetic (TM)* A_r waves. Both vector potentials are solutions to the Helmholtz equation [14, ch.6-1] and can be used to find the fields in all four region. In the paper the fields will be expressed in terms of the TE modes only since the TM modes are smaller in comparison. The problem starts with the assumption that there is a localized (i.e. assumed as a delta function) radiating magnetic field in region (3) at a distance r_s coming from the direction (θ_s,φ_s) (the subscript s denotes source). Since the H-field is localized it can be described by the following equation which.

$$\bar{H}_s = \hat{\theta}H_o\delta(\theta-\theta_s)\delta(\varphi-\varphi_s)+\hat{\varphi}H_o\delta(\theta-\theta_s)\delta(\varphi-\varphi_s) \tag{1}$$

Where H_o represents the magnitude of the H-field. To solve the BVP equation (1) must be expanded in terms of the TE modes as shown in (2):

$$\bar{H}_s = -i\sqrt{\frac{\varepsilon_3}{\mu_0}}\sum_{l=1}^{\infty}\sum_{m=-l}^{l}F_{lm}\nabla\times\left[j_l(k_3r)\bar{r}\times\nabla Y_{lm}(\theta,\varphi)\right]\big|_{r=r_s} \tag{2}$$

To find the coefficient F_{lm} of the TE expansion (1) and (2) are equated and then the orthogonality property of the TE modes is applied. F_{lm} is given by the following equation.

$$F_{lm} = \frac{k_3 r_s \sqrt{\mu_o} / J_l'(k_3 r_s)}{i\sqrt{\varepsilon_3}\, l(l+1)} \left[\sin\theta_s \frac{\partial Y_{lm}^*(\theta_s,\varphi_s)}{\partial\theta} - imY_{lm}^*(\theta_s,\varphi_s) \right] \tag{3}$$

Where $J(k_3r) = k_3 r j_l(k_3r)$ and $j_l(k_3r)$ [14, ch.6-1] is the spherical Bessel function, J_l' is the derivative w.r.t r, $i = \sqrt{-1}$, μ_0 is the permeability of free space, ϵ_3 is the relative permittivity of region (3) and $Y_{lm}(\theta, \varphi)$ is the spherical harmonic with l and m as the indices of the expansion. The wavenumber k_3 is given by:

$$k_3 = \omega\sqrt{\mu_0\varepsilon_0(\varepsilon_3 + \frac{i\sigma_3}{\omega\varepsilon_0})} \tag{4}$$

Where ε_0 is the permittivity of free space, $\omega = 2\pi f$ is the frequency in radian/sec (f=*500kHz*) and σ_3 is the conductivity of region (3).

Beginning with the field in region (3) as the source, one can use the boundary conditions presented in (5)-(10) to solve for the current density of each antenna element given by (8).

$$\hat{r}\times(\vec{E}_1 - \vec{E}_0) = 0 \text{ for } r = c \tag{5}$$

$$\hat{r}\times(\vec{E}_2 - \vec{E}_1) = 0 \text{ for } r = b \tag{6}$$

$$\hat{r}\times(\vec{E}_3 - \vec{E}_2) = 0 \text{ for } r = a \tag{7}$$

$$\hat{r}\times(\vec{H}_1 - \vec{H}_0) = \vec{J}_i(\theta,\varphi) \text{ for } r = c \tag{8}$$

$$\hat{r}\times(\vec{H}_2 - \vec{H}_1) = 0 \text{ for } r = b \tag{9}$$

$$\hat{r}\times(\vec{H}_3 - \vec{H}_2) = 0 \text{ for } r = a \tag{10}$$

Where $\boldsymbol{H}_j$ and $\boldsymbol{E_j}$ represent the magnetic intensity (H-field) and electric field in the region (j) and $\boldsymbol{J_i}$ is the current density of the i-th antenna element.

By solving the BVP by using equation (2) and (5)-(10), one can derive the expression of the current density induced at the ith antenna. After determining the current density it is very easy to determine the current signal induced at the ith antenna and this is given by (11).

$$I_i = L\sum_{l=1}^{\infty}\sum_{m=-l}^{l} F_{lm}\Psi_l \frac{im}{\sin\theta_i} Y_{lm}(\theta_i,\varphi_i) \tag{11}$$

Where:

$$\Psi_l = \frac{\eta_0}{k_0 c}\frac{H_l^{'(2)}(k_0 c)}{H_l^{(2)}(k_0 c)}\left\{H_l^{(1)}(k_1 c)\left[\frac{\tau_l J_l(k_3 a)}{\gamma_l H_l^{(1)}(k_2 a)+H_l^{(2)}(k_2 a)}\right]+\right.$$
$$\left.H_l^{(2)}(k_1 c)\left[\frac{J_l(k_3 a)}{H_l^{(2)}(k_1 b)}\left[\frac{\gamma_l H_l^{(1)}(k_2 b)+H_l^{(2)}(k_2 b)-\tau_l H_l^{(1)}(k_1 b)}{\gamma_l H_l^{(1)}(k_2 a)+H_l^{(2)}(k_2 a)}\right]\right]\right\}$$
$$-\frac{\eta_1}{k_1 c}\frac{\tau_l J_l(k_3 a) H_l^{'(1)}(k_1 c)}{\gamma_l H_l^{(1)}(k_2 a)+H_l^{(2)}(k_2 a)}$$
$$-\frac{\eta_1}{k_1 c}\frac{J_l(k_3 a) H_l^{'(2)}(k_1 c)}{H_l^{(2)}(k_1 b)}\left[\frac{\gamma_l H_l^{(1)}(k_2 b)+H_l^{(2)}(k_2 b)-\tau_l H_l^{(1)}(k_1 b)}{\gamma_l H_l^{(1)}(k_2 a)+H_l^{(2)}(k_2 a)}\right] \quad (12)$$

$$\gamma_l = \frac{H_l^{'(2)}(k_2 a) J_l(k_3 a) - H_l^{(2)}(k_2 a) J_l^{'}(k_3 a)}{H_l^{(1)}(k_2 a) J_l^{'}(k_3 a) - H_l^{'(1)}(k_2 a) J_l(k_3 a)}$$

$$\tau_l = \frac{\left\{\begin{array}{l}\left[\gamma_l H_l^{(1)}(k_2 b)+H_l^{(2)}(k_2 b)\right] H_l^{'(2)}(k_1 b)\\ -\left[\gamma_l H_l^{'(1)}(k_2 b)+H_l^{'(2)}(k_2 b)\right] H_l^{(2)}(k_1 b)\end{array}\right\}}{\left[H_l^{(1)}(k_1 b) H_l^{'(2)}(k_1 b) - H_l^{'(1)}(k_1 b) H_l^{(2)}(k_1 b)\right]} \quad (13)$$

Where L is the dimension of the antenna element, $H_l^{(1,2)}(k,r) = krh_l^{(1,2)}(k,r)$ and $h_l^{(1,2)}(k,r)$ [14, ch.6-1] is the spherical Hankel function of the first and second kind and $H_l^{'}$ is the derivative w.r.t r. The coefficients presented in (12) and (13) are simply the result from solving the BVP.

2.2 Beamforming Technique

After obtaining the received current signal equation in the previous section it is now possible to consider the beamforming technique that will allow the array to efficiently scan the environment. By proper scanning the array will determine the source from which the source H-field originated.

The idea behind the technique is based on the orthogonality principle of the TE modes. To begin the analysis the received input current at the ith antenna element is expressed as follows.

$$I_{it} = I_i + n_i \quad (14)$$

Where I_i is given by (11) and n_i is a zero mean white Gaussian noise. Each signal I_i will be multiplied by a weight factor (i.e. magnitude and phase) g_i and then all the signals from all the elements are added up to produce one output current I_{out} given by equation (15).

$$I_{out} = \sum_{i=1}^{N} I_{it} g_i = \sum_{i=1}^{N}\left(I_i g_i + n_i g_i\right) = FSg^V + Ng^V \quad (15)$$

The first part of (15) gives the output current in a summation form while the second part expresses the current in a matrix form.

Where:

$$F = \begin{bmatrix} F_{1,-1}(\theta_s,\varphi_s) & F_{1,0}(\theta_s,\varphi_s) & F_{1,1}(\theta_s,\varphi_s) & . & . & F_{M,M}(\theta_s,\varphi_s) \end{bmatrix} \tag{16}$$

$$g^V = \begin{bmatrix} g_1 \\ g_2 \\ g_3 \\ . \\ . \\ g_N \end{bmatrix} \tag{17}$$

$$S = \begin{bmatrix} \Psi_1 \frac{-j}{\sin\theta_1} Y_{1,-1}(\theta_1,\varphi_1) & \Psi_1 \frac{-j}{\sin\theta_2} Y_{1,-1}(\theta_2,\varphi_2) & . & . & . & \Psi_1 \frac{-j}{\sin\theta_N} Y_{1,-1}(\theta_N,\varphi_N) \\ 0 & 0 & . & . & . & 0 \\ \Psi_1 \frac{j}{\sin\theta_1} Y_{1,1}(\theta_1,\varphi_1) & \Psi_1 \frac{j}{\sin\theta_2} Y_{1,1}(\theta_2,\varphi_2) & . & . & . & \Psi_1 \frac{j}{\sin\theta_N} Y_{1,1}(\theta_N,\varphi_N) \\ . & . & & . & & . \\ . & . & & . & & . \\ \Psi_M \frac{jM}{\sin\theta_1} Y_{M,M}(\theta_1,\varphi_1) & \Psi_M \frac{jM}{\sin\theta_2} Y_{M,M}(\theta_2,\varphi_2) & . & . & . & \Psi_M \frac{jM}{\sin\theta_N} Y_{M,M}(\theta_N,\varphi_N) \end{bmatrix} \tag{18}$$

$$N = \begin{bmatrix} n_1 & n_2 & n_3 & . & . & n_N \end{bmatrix} \tag{19}$$

F is a vector that contains the information about the source signal, S is a matrix that contains the terms of the double sum present in (11), g^V is a column vector that contains the adjustable weights and N is a row vector that contains the noise for each antenna element.

The aim in this problem is to use the vector g^V to transfer the matrix S into the following desired vector.

$$S_{Desired} = \begin{bmatrix} \frac{-j}{\sin\theta} Y_{1,-1}(\theta,\varphi) \\ 0 \\ \frac{j}{\sin\theta} Y_{1,1}(\theta,\varphi) \\ . \\ . \\ \frac{jM}{\sin\theta} Y_{M,M}(\theta,\varphi) \end{bmatrix} \tag{20}$$

Reducing the matrix from S to the vector $S_{Desired}$ allows for the use of the orthogonality principle. When considering the product between F and $S_{Desired}$ the output current becomes:

$$I_{out} = FS_{Desired} + Ng^V = \sum_{l=1}^{M=7}\sum_{m=-l}^{l} F_{lm}\frac{jm}{\sin\theta}Y_{lm}(\theta,\varphi) + \sum_{i=1}^{N} n_i g_i$$
$$I_{out} \approx \delta(\theta-\theta_s)\delta(\varphi-\varphi_s) + \sum_{i=1}^{N} n_i g_i \tag{21}$$

It is clear from (21) that the resulting current is desired to be a delta-like form in the control angles (θ, φ) with some added noise. The scanning process is done in the sense that the control angles (θ, φ) are going to be varied from 0 to π for θ and from 0 to 2π for φ. For each control angle set (θ, φ), I_{out} is calculated by first finding the optimal set of weight factors g^V. When the calculation is done for all the angle sets, plotting $I_{out}(\theta, \varphi)$ will show that the output will have its maximum value at (θ_s, φ_s) which is the aim of the array. In this way by using some kind of a maximum seeking circuit and after that determining at which control angle set this maximum was found, the direction of arrival detection is possible.

To transform S to $S_{Desired}$ the following problem must be solved for each control angle set.

$$\arg\min_g \left\| Sg^V - S_{Desired} \right\|^2 \tag{22}$$

The above minimization statement can be easily solved for with respect to the vector g^V by setting the vector to:

$$g_{opt}^V = (S^H S)^{-1} S^H S_{Desired} \tag{23}$$

Note that the same analysis applies if more than one source is being detected.

3 Matlab Simulation Results

The theory presented in Section II is simulated in MATLAB. As mentioned earlier 42 elements were used in the simulation. Each element has a dimension of L=*2cm* and the frequency of reception is taken to be 500 kHz. The spacing between the centers of the elements is ≈ 4 cm. For an operating frequency of 500 kHz the electromagnetic properties of the human head in region 0-3 are as follows (as given in [15]): region (0) has the free space permittivity and permeability; region (1) has $\varepsilon_1 = 38.87\epsilon_0$, $\mu_1 = \mu_0$ & $\sigma_1 = 1.88$S/m; region (2) has $\varepsilon_2 = 19.34\epsilon_0$, $\mu_2 = \mu_0$ & $\sigma_2 = 0.59$S/m; and region (3) has $\varepsilon_3 = 51.8\epsilon_0$, $\mu_3 = \mu_0$ & $\sigma_3 = 1.5$S/m. The simulations in Figures 3-5 show how the output current I_{out} in (21) varies with the angular parameters θ and φ. Note that all the simulations made are for a radial distance of $r_{(0)} = 5$ cm from the center of the coordinate system as shown in Fig. 1.

It is clear from the figures that the beamforming technique is successful in determining the direction of the source H-field (θ, φ) indicated by each figure. The origin of the source clearly corresponds to the maximum value in the output current at every case. For the case of Fig. 5b it is clear that the technique is

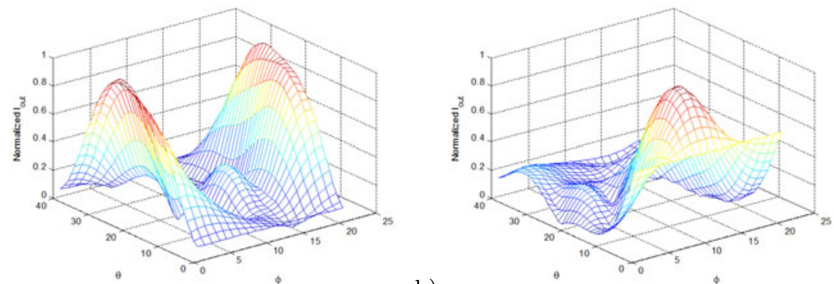

a) b)

Fig. 3. *a)* $I_{out}(\theta, \varphi)$ for $\theta_s = \frac{\pi}{2}$ & $\varphi_s = 0$. *b)*$I_{out}(\theta, \varphi)$ for $\theta_s = \frac{\pi}{4}$ & $\varphi_s = \pi$

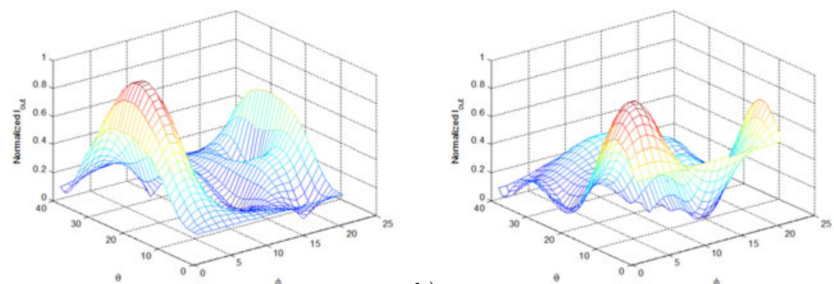

a) b)

Fig. 4. *a)* $I_{out}(\theta, \varphi)$ for $\theta_s = \frac{\pi}{4}$ & $\varphi_s = \frac{\pi}{2}$. *b)*$I_{out}(\theta, \varphi)$ for $\theta_s = \frac{\pi}{2}$ & $\varphi_s = \frac{\pi}{4}$

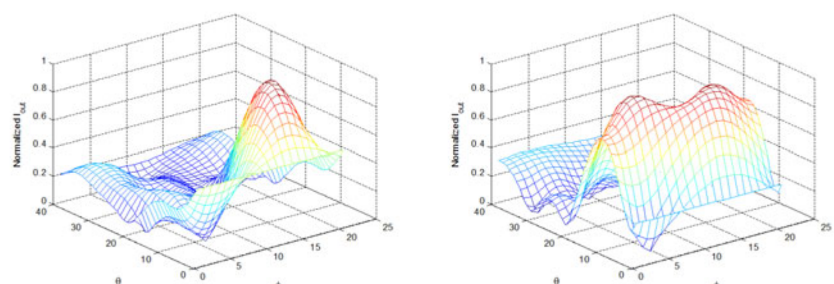

a) b)

Fig. 5. *a)* $I_{out}(\theta, \varphi)$ for $\theta_s = \frac{\pi}{4}$ & $\varphi_s = \frac{3\pi}{2}$. *b)*$I_{out}(\theta, \varphi)$ for $\theta_{s1} = \frac{\pi}{4}$ & $\varphi_{s1} = \frac{3\pi}{2}$ *and* $\theta_{s2} = \frac{\pi}{4}$ & $\varphi_{s2} = \frac{\pi}{2}$

applicable for multiple source detection (in this example two sources). It is clear from Fig. 5b that there are two maximum values for the current which correspond to the two location of the two source H-fields. Another remark is the scaling used in the figures. The simulation was carried out for values of θ ranging from 0 to π and φ ranging from 0 to 2π. In the plots the θ range is divided into 40 points while the φ range is divided into 20 points. For example, for the φ-axis the point 10 corresponds to $\varphi = 10 * \frac{2\pi}{20} = \frac{\pi}{2}$ and for the θ axis the same point corresponds to $\theta = 10 * \frac{\pi}{40} = \frac{\pi}{4}$.

4 Conclusions and Future Work

A theoretical hemispherical antenna array is designed and simulated to receive brain waves or signals embedded in the human head. A new beamforming technique that makes use of the orthogonality property of the TE modes is devised and used. The beamforming technique used is successful in receiving from single or multiple sources. The array can be applied to any other application where spherical geometry is involved where the task is to receive signals from within this spherical geometry. The maximum seeking circuit for the output current is under investigation and also the antenna elements and all the radio-frequency RF front-end circuitry is being designed for simulation.

References

[1] Want, R.: An Introduction to RFID Technology. In: IEEE CS and IEEE ComSoc. (2006)
[2] Rueangsi, N., Thanachayanont, A.: Coil Design for Opt imum Operating Range of Magnetically-Coupled RFID System. In: IEEE ISCIT, pp. 1199–1202 (2006)
[3] Atluri, S., Ghovanloo, M.: Incorporating Back T elemet ry in a Full-Wave CMOS Rect ifier for RFID and Biomedical Applicat ions. IEEE, Los Alamitos (2007)
[4] Fotopoulou, K., Flynn, B.: Optimum Antenna Coil Structure for Induct ive Powering of Passive RFID Tags. In: IEEE International Conference in RFID, pp. 71–77 (2007)
[5] Amin, M., Rahman, A., Bin-Mahbub, S., Ahmed, K., Chowdhury, Z.: Estimat ion of Direct ion of Arrival (DOA) Using Real-T ime Array Signal Processing. In: 5th International Conference on Electrical and Computer Engineering ICECE 2008, Dhaka, Bangladesh, December 20-22, pp. 422–427 (2008)
[6] Vasylyshyn, V.I.: Antenna Array Signal Processing with High -Resolution By Modified Beamspace Music Algorithm. In: International Conference on Antenna Theory and Techniques, Sevastopol, Ukraine, September 17-21, pp. 455–457 (2007)
[7] Zooghby, A., Christodoulou, C.C., Georgiopoulos, M.: A Neural Network-Based Smart Antenna for Multiple Source Tracking. IEEE Transaction on Antennas and Propagation 48(5), 768–776 (2000)
[8] Sarevska, M., Milovanovic, B.: Alternative Signal Detection For Neural Network-Based Smart Antenna. In: 7th Seminar on Neural Network Applications in Electrical Engineering, Neural-2004, September 23–25, pp. 85–89 (2004)
[9] Sarevska, M., Salem, A.: Antenna Array Beamforming using Neural Network. World Academy of Science, Engineering and Technology 24, 115–119 (2006)
[10] Caylar, S., Dural, G., Leblebicioglu, K.: Neural Network Method for Direction of Arrival Estimation with Uniform Cylindrical Microstrip Patch Array. IET Microwaves, Antennas &Propagation (2008)
[11] Svantesson, T., Wennstrom, M.: High Resolution Direction Finding Using a Switched Parasitic Antenna,
`http://www.signal.uu.se/Publications/pdf/c0111.pdf`

[12] Chen, H.H., Chan, S.C., Zhang, Z.G., Ho, K.L.: Adaptive Beamforming and Recursive DOA Estimation Using Frequency-Invariant Uniform Concentric Spherical Spheres. IEEE Transactions on Circuit and Systems 55(10), 3077–3089 (2008)
[13] Allen, B., Ghavami, M.: Adaptive Array Systems. Wiley, Chichester (2005)
[14] Harrington, R.F.: Time-Harmonic Electromagnetic Fields. In: IEEE Press Series on Electromagnetic Wave Theory, ch. 6, pp. 264–269 (2001)
[15] Marinova, I., Mateev, V.: Electromagnetic Field Modeling in Human Tissue. World Academy of Science, Engineering and Technology 64, 298–303 (2010)
[16] Partal, P., Mautz, R., Arvas, E.: Radiation from a Circular Loop in the Presence of a Spherically Symmetric Conducting or Dielectric Objects. IEEE Trans. Antenna and Propagation 48(10), 1646–1652 (2000)
[17] Li, Z., Duraiswami, R.: Flexible and Optimal Design of Spherical Microphone Arrays for Beamforming. IEEE Trans. Speech & Audio Processing 15(2), 702–714 (2007)